Naval Research Laboratory

Washington, DC 20375-5320

NRL/MR/6720--20-10,194

Characterization of Electron Beams from a Dense Plasma Focus

Emil Petkov

Radiation Hydrodynamics Branch
Plasma Physics Division (Former)

L3Harris, Applied Technologies Inc.
San Leandro, CA

Stuart Jackson

Pulsed Power Physics Branch
Plasma Physics Division

Andrey Beresnyak
Arati Dasgupta

Radiation Hydrodynamics Branch
Plasma Physics Division

February 15, 2021

REPORT DOCUMENTATION PAGE

Form Approved
OMB No. 0704-0188

1. REPORT DATE *(DD-MM-YYYY)*	**2. REPORT TYPE**	**3. DATES COVERED** *(From - To)*
15-02-2021	NRL Memorandum Report	June 2018 – June 2020

4. TITLE AND SUBTITLE

Characterization of Electron Beams from a Dense Plasma Focus

5a. CONTRACT NUMBER

5b. GRANT NUMBER

5c. PROGRAM ELEMENT NUMBER
NISE

6. AUTHOR(S)

Emil Petkov*, Stuart Jackson, Andrey Beresnyak, and Arati Dasgupta

5d. PROJECT NUMBER

5e. TASK NUMBER

5f. WORK UNIT NUMBER
N2P6

7. PERFORMING ORGANIZATION NAME(S) AND ADDRESS(ES)

Naval Research Laboratory
4555 Overlook Avenue, SW
Washington, DC 20375-5320

8. PERFORMING ORGANIZATION REPORT NUMBER

NRL/MR/6720--20-10,94

9. SPONSORING / MONITORING AGENCY NAME(S) AND ADDRESS(ES)

Naval Research Laboratory
4555 Overlook Avenue, SW
Washington, DC 20375-5320

10. SPONSOR / MONITOR'S ACRONYM(S)

NRL-NISE

11. SPONSOR / MONITOR'S REPORT NUMBER(S)

12. DISTRIBUTION / AVAILABILITY STATEMENT

DISTRIBUTION STATEMENT A: Approved for public release; distribution is unlimited.

13. SUPPLEMENTARY NOTES

*L3Harris, Applied Technologies Inc., 2700 Merced St., San Leandro, CA 94577
*Former Plasma Physics Division

14. ABSTRACT

Research was conducted in an effort to study the physics of high-energy electron beams generated in a dense plasma focus (DPF). The effort consisted of both theoretical and experimental approaches. Theoretical calculations were performed using various non-local thermodynamic equilibrium (non-LTE) kinetic models to identify line candidates that would exhibit a measureable degree of polarization. Experiments carried out on Hawk tested different gases in the gas-puff nozzle at varying pressures. A convex crystal spectrometer was benchmarked using different crystals and filters, and was mounted on the Hawk chamber for collection of spectroscopic data. This memorandum summarizes the overall results of the project.

15. SUBJECT TERMS

Dense plasma focus Spectroscopy
Non-LTE modeling

16. SECURITY CLASSIFICATION OF:			**17. LIMITATION OF ABSTRACT**	**18. NUMBER OF PAGES**	**19a. NAME OF RESPONSIBLE PERSON**
a. REPORT	**b. ABSTRACT**	**c. THIS PAGE**			Emil Petkov
Unclassified Unlimited	Unclassified Unlimited	Unclassified Unlimited	Unclassified Unlimited	17	**19b. TELEPHONE NUMBER** *(include area code)* (202) 404-7721

Standard Form 298 (Rev. 8-98)
Prescribed by ANSI Std. Z39.18

This page intentionally left blank.

CONTENTS

FIGURES

TABLES

1. EXECUTIVE SUMMARY

Research was conducted in an effort to study the physics of high-energy electron beams generated in a dense plasma focus (DPF). The effort consisted of both theoretical and experimental approaches. Theoretical calculations were performed using various non-local thermodynamic equilibrium (non-LTE) kinetic models to identify line candidates that would exhibit a measureable degree of polarization. A finite-volume magnetohydronamics (MHD) code was used to estimate what plasma temperature and density can be achieved from plasma produced by a DPF driven by NRL's Hawk pulsed-power generator. The experiments carried out on Hawk tested different gases in the gas-puff nozzle at varying pressures. A convex crystal spectrometer was benchmarked using different crystals and filters, and was mounted on the Hawk chamber for collection of spectroscopic data. This memorandum summarizes the overall results of the project.

Several K-shell emission lines from helium-like (He-like) and hydrogen-like (H-like) argon and neon were considered as candidates for plasma polarization spectroscopy (PPS). Calculations performed using the Flexible Atomic Code under conditions which would provide maximum polarization show that the He-α resonance line ($1s2p\ ^1P_1 \rightarrow 1s^2\ ^1S_o$), He-α intercombination line ($1s2p\ ^3P_1 \rightarrow 1s^2\ ^1S_o$), and He-β resonance line, ($1s3p\ ^1P_1 \rightarrow 1s^2\ ^1S_o$) are useful candidates from the He-like shell. From the H-like shell, the Ly-α doublet lines ($2p\ ^2P_{3/2} \rightarrow 1s\ ^2S_{1/2}$ and $2p\ ^2P_{3/2} \rightarrow 1s\ ^2S_{1/2}$) are the best line candidates. The collisional-radiative spectral analysis code PrismSPECT was used to calculate K-shell radiative cooling rates. These were fed into the MHD code Athena which estimated sufficiently high plasma and ion densities from a Hawk shot with deuterium in the Marshall guns and argon or neon as a dopant in the gas-puff nozzle. A magnetic sublevel kinetics code was developed to complement experimental efforts. The code is capable of handling a two-temperature electron distribution function (EDF) where one temperature represents the thermal electrons, and the other represents the non-thermal electrons. Visible spectroscopy of experiments on Hawk with argon in the gas-puff nozzle indicated lines from impurities as well as singly ionized argon. Due to the Covid-19 pandemic, the experimental measurements of the electron temperature and density, as well as the development of the two-crystal spectropolarimeter were indefinitely delayed.

This page intentionally left blank.

2. BACKGROUND

A dense plasma focus is a system used for the generation of high-energy-density (HED) plasmas. It can be operated as a source for either neutrons [1] or high energy x-rays [2]. During its operation, a rapidly changing magnetic field quickly collapses and induces the formation of an electric field. This field accelerates a beam of highly energetic electrons in one direction. A detailed study of the electron beam generation will address the longstanding question in fundamental physics of what underlying physical mechanisms lead to the formation of electron beams in pinched plasmas. Understanding of this mechanism may enable the production of high energy x-rays at a level required for radiation hardness testing of electronic systems. One way to investigate the electron distribution function (EDF) and fields within plasma is to use plasma polarization spectroscopy (PPS). This novel diagnostic tool is applicable across plasmas of very different densities, from low-density astrophysical plasmas to high-density z-pinch plasmas. It relies on coupling sophisticated atomic and ionization modeling with analysis of emission data obtained with a specially designed spectrometer. This technique is considered here for the energetic electron beams generated in a DPF driven by NRL's Hawk pulsed-power generator.

2.1 Scientific Goals

In order to improve our understanding of electron beam generation from a DPF, a combination of sophisticated simulations as well as experimental data must be generated. The work here focused first on identifying suitable line-emission candidates for plasma polarization spectroscopy. A multitude of theoretical tools were employed to this purpose. The Flexible Atomic Code [3] was utilized for all calculations of atomic data, including transition energies, collisional excitation cross sections, and radiative decay rates. This code can also be used to estimate the polarization of a line-candidate assuming an EDF which would maximize the degree of polarization. Since the plasma produced in a DPF consists of a relatively small percentage of non-thermal electrons, and thus mostly consist of thermal electrons, a new code was developed to calculate the degree of polarization of the line candidates using a two-temperature EDF. The new code is also capable of producing polarization sensitive synthetic spectra.

The experimental goals of this research consisted of several components. A visible spectrometer was used as a diagnostic to ensure that the gas-puff valve was injecting dopant into the chamber. A finite-volume MHD code was also used to estimate the plasma temperature and density that would be achieved in a configuration where deuterium plasma was injected via Marshall guns, and the plasma was doped with a small amount of argon. A convex crystal spectrometer was used as the primary diagnostic to record time-integrated, spatially resolved spectra. An x-ray pinhole camera was used as a diagnostic to evidence the pinching of the plasma within the chamber. This spectrometer was benchmarked and tested off-line using a small x-ray pulser. Subsequent spectroscopic measurements would have been used as a proof-of-principle x-ray spectrometer design that will then be duplicated in a second spectrometer. These two spectrometers would be used as a pair, with their diffractive crystals oriented such that one spectrometer records x-rays polarized parallel and the other perpendicular to the direction of propagation of the electron beam produced in the DPF plasma.

Manuscript approved February 4, 2021.

2.2 Technical Approach

This research project combined theoretical and experimental efforts. On the theoretical front, it was necessary to first determine suitable line candidates for polarization spectroscopy. This technique requires that spectroscopic measurements record at least two x-ray emission lines. Ideally, one of the lines will be intrinsically unpolarized for cross-normalization purposes. If there is no line which has zero polarization, the next best candidate is a line which has a low degree of polarization. The degree of polarization must also remain relatively flat as a function of the electron impact energy. The dopant added in the proposed experiments cannot be too heavy, thus neon and argon are good element choices. To determine the line candidates, the polarization module of FAC was utilized. This module allows one to calculate line polarization due to collisional excitation by electron impact. The module assumes a Gaussian EDF and takes into account radiative cascade effects. Thus the resulting calculations present an ideal-case scenario. In reality, the EDF generated in a DPF driven by NRL's Hawk pulsed-power generator will consist largely of thermal electrons with a small tail of non-Maxwellian electrons. To this effect, a new code was developed which can take a two-temperature EDF and produce polarization sensitive synthetic spectra. The code uses atomic data generated using FAC for the magnetic sublevels of the selected configurations. The degree of polarized line emission is then calculated based on this atomic kinetics model. The degree of polarization is given by,

$$P = \frac{I_{||} - I_{\perp}}{I_{||} + I_{\perp}} \tag{1}$$

where $I_{||}$ and $I_{\perp}$ are the electric field vector intensities that are parallel and perpendicular to the electron beam direction. Assuming that the plasma is optically thin, these intensities can be represented by,

$$I_{\parallel,\perp} = h\nu A\left(J_i \longrightarrow J_f\right) \times \sum_{M_i=-J_i}^{J_i} f(M_i) \sum_{M_f=-J_f}^{J_f} MI_{\parallel,\perp}(\Delta M, \vartheta = 90^{\circ}) \times \left(J_f q M_f - \Delta M | J_i M_i\right)^2 \tag{2}$$

where $h\nu$ is the energy of the transition, $A\left(J_i \longrightarrow J_f\right)$ is the radiative decay rate of the transition, $f(M_i)$ are the populations of the upper magnetic sublevels, and $MI_{\parallel,\perp}$ are the relative multiple intensities. The last term in the parenthesis is the Clebsch-Gordan coefficient. The product of this term and the radiative decay rate yields the radiative decay rates of the fine-structure levels via application of the Wigner-Eckart theorem. The magnetic sublevel populations are calculated by solving a system of kinetic rate equations given by $\boldsymbol{Af = b}$ where $\boldsymbol{A}$ is the rate matrix, $\boldsymbol{f}$ is the vector with magnetic sublevel populations, and $\boldsymbol{b}$ is the rate vector. The candidates considered in this research were electric dipole (E1) transitions, and the final expression for their polarization can be expressed, in terms of the magnetic sublevel populations, as

$$P = -\frac{f(-1) - 2f(0) + f(+1)}{f(-1) + 2f(0) + f(+1)} \tag{3}$$

After determining suitable line candidates, it is necessary to make estimates of the plasma temperature and density that can be achieved in a DPF shot driven by the Hawk pulsed-power generator. For this effort, the collisional-radiative spectral analysis code PrismSPECT was used to calculate the radiative K-shell cooling rates of argon plasma. The cooling rates were then fed into

the finite volume MHD code known as Athena [4]. This finite volume MHD code is based on approximate Riemann solvers.

The experiments conducted for this research effort consisted of DPF loads driven by the Hawk pulsed-power generator. Hawk is capable of delivering up to 680 kA of current with a 1.2 μs rise time into this type of load. Whereas most other DPF banks have low inductance (typically 10's of nH), Hawk has an unusually high inductance (607 nH). The higher inductance has led to speculation that Hawk may be able to drive implosions beyond their typical load conditions, and thus is being investigated at NRL, in general, as a testbed to study mechanisms of charged particle acceleration. During typical operation, a current pulse is initiated in plasma that is injected with three Marshall guns [5] in the coaxial spaces between the electrodes. A gas-puff valve recessed inside the center conductor is used to add dopants such as Ne or Ar. A general schematic of the Hawk Marx bank and the load chamber is given in Fig 1.

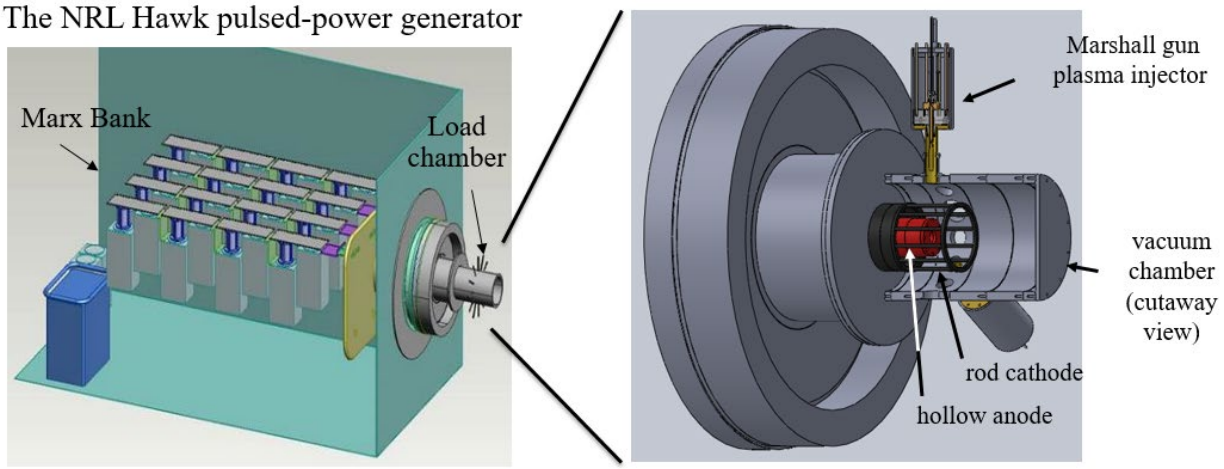

Fig. 1 An illustration of the Hawk Marx bank and the load chamber. Three Marshall guns are used to inject deuterium plasma. The Marshall guns are approximately 1 cm upstream from the end of the center conductor. The center gas-puff valve is used to add additional gaseous dopants.

A visible spectrometer was used as a diagnostic to test whether sufficient dopant makes it into the chamber. A convex crystal spectrometer is the primary diagnostic mounted on the Hawk chamber for recording time-integrated spatially-resolved spectra. The spectrometer was tested with both KAP and mica crystals. A general setup and mechanism of action of the spectrometer is illustrated in Fig 2.

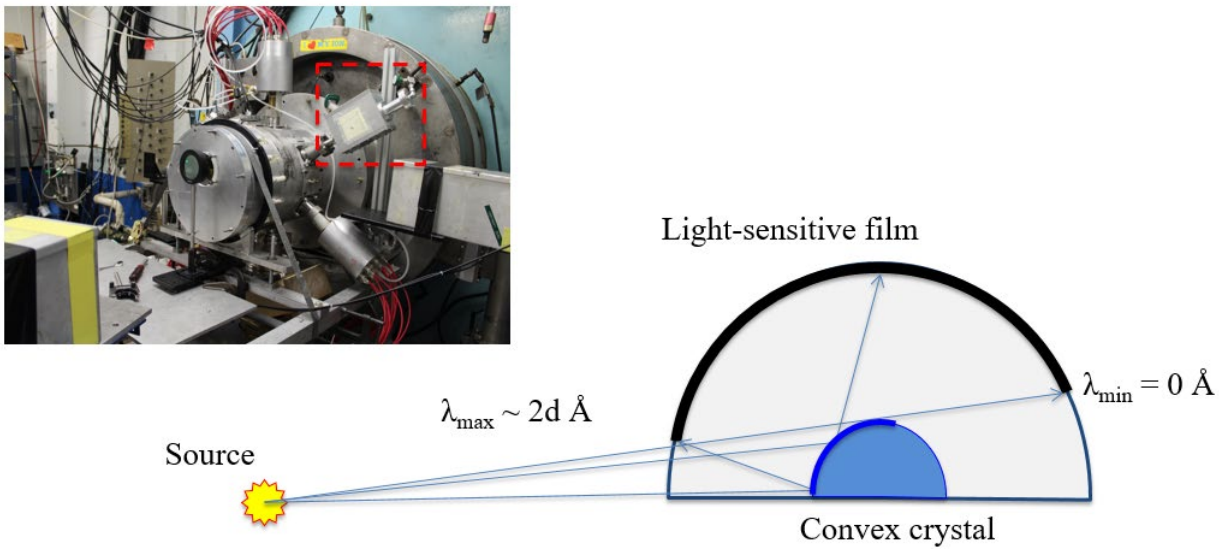

Fig. 2 The convex crystal spectrometer and its mounting location on the Hawk chamber.

The crystal spectrometer diffracts x-ray spectral lines according to Bragg's Law.

$$n\lambda = 2dsin\theta \quad (4)$$

In equation (4), n is the order of diffraction, λ is the wavelength of the diffracted light, θ is the Bragg angle, and d is the interplanar lattice spacing of the crystal. The maximum wavelength that can be diffracted by the spectrometer is approximately equal to twice the interplanar lattice spacing. For polarization spectroscopy, a crystal should be selected which yields a nominal Bragg angle as close to 45° as possible for the selected lines of interest. The reflectivity of most crystals varies roughly as $\cos^2(\theta)$, therefore at 45° a spectrometer can be tuned to selectively pick up only one component of the electric field vector intensities. Two x-ray pinhole cameras are placed 1 cm upstream of the end of the center conductor and are used to image the resulting plasma.

2.3 Results

The details of the theoretical efforts are summarized first. The non-local thermodynamic equilibrium (non-LTE) codes SUNR [6], PrismSPECT, and Drachma-II [7] were used to calculate the wavelengths of several transitions of interest, as well as to produce synthetic spectra of these transitions. Figure 3 shows a sample synthetic spectrum produced using the aforementioned codes as well as the calculated ionization balance from each code. Each spectrum was simulated using an electron temperature T_e = 1500 eV and an electron density $n_e = 1x10^{19}cm^{-3}$. The most intense He-like and H-like lines are labeled. Table I lists the ion lines, their transitions, and respective wavelengths.

Table 1 – Theoretical values of wavelengths (λ in Å) of select He-like and H-like lines of Ar.

Ion Line	Transition	λ[Å] SCRAM	λ[Å] PrismSPECT	λ[Å] Drachma-II
He α-IC	$1s2p\ ^3P_1 \rightarrow 1s^2\ ^1S_0$	3.971	3.969	3.970
He α	$1s2p\ ^1P_1 \rightarrow 1s^2\ ^1S_0$	3.950	3.949	3.949
Ly α2	$2p\ ^2P_{1/2} \rightarrow 1s\ ^2S_{1/2}$	3.736	3.737	3.736
Ly α1	$2p\ ^2P_{3/2} \rightarrow 1s\ ^2S_{1/2}$	3.731	3.731	3.731
He β	$1s3p\ ^1P_1 \rightarrow 1s^2\ ^1S_0$	3.367	3.366	3.367

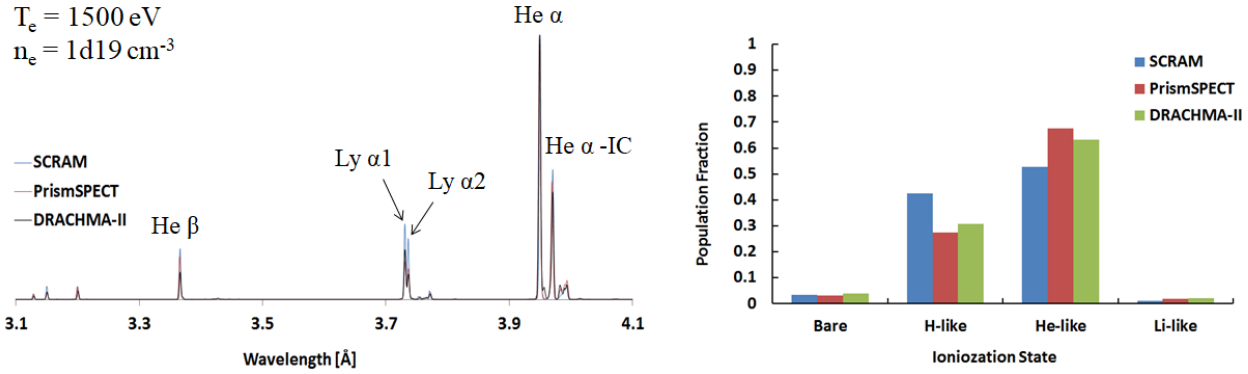

Fig. 3 Synthetic spectra (left image) of K-shell Ar radiation produced using several non-LTE codes. The calculated ionization balance (right image) from each code is also shown.

The most intense He-like lines correspond to the He-α, He-α IC, and He-β transitions. The most intense H-like lines correspond to the Ly-α1 and Ly-α2 lines, commonly referred to as the Ly-α doublet. Several criteria should be considered when selecting line candidates for polarization spectroscopy. First, the lines should have sufficiently high intensity such that they can be picked up by the spectroscopic diagnostic. Moreover, depending on the resolving power of available crystals, the lines should be somewhat spaced from each other. The results shown in Fig. 3 indicate that in terms of relative spacing and intensity, the He-α, He-α IC, and He-β may be useful candidates. In order to use the Ly-α doublet, one would need a spectrometer with a crystal that provides very high resolution. However, in the following discussion, the usefulness of these two lines will be highlighted, despite their minimal spacing.

The next step in determining the suitability of the aforementioned lines for PPS is to perform calculations to determine their degree of polarization. The polarization module of FAC was used for this task. In this module, the configurations of interest were explicitly chosen to produce the lines of interest mentioned above. The module then calculates the degree of polarization of the x-ray emission lines due to collisional excitation with electrons in a Gaussian EDF. This is an idealized scenario since the fraction of non-thermal electrons in this case is considered to be 100%. Figure 4 illustrates the values of the degree of polarization. The

polarization was calculated for several electron impact energies ranging from near threshold energy (around 3 keV) up to 50 keV.

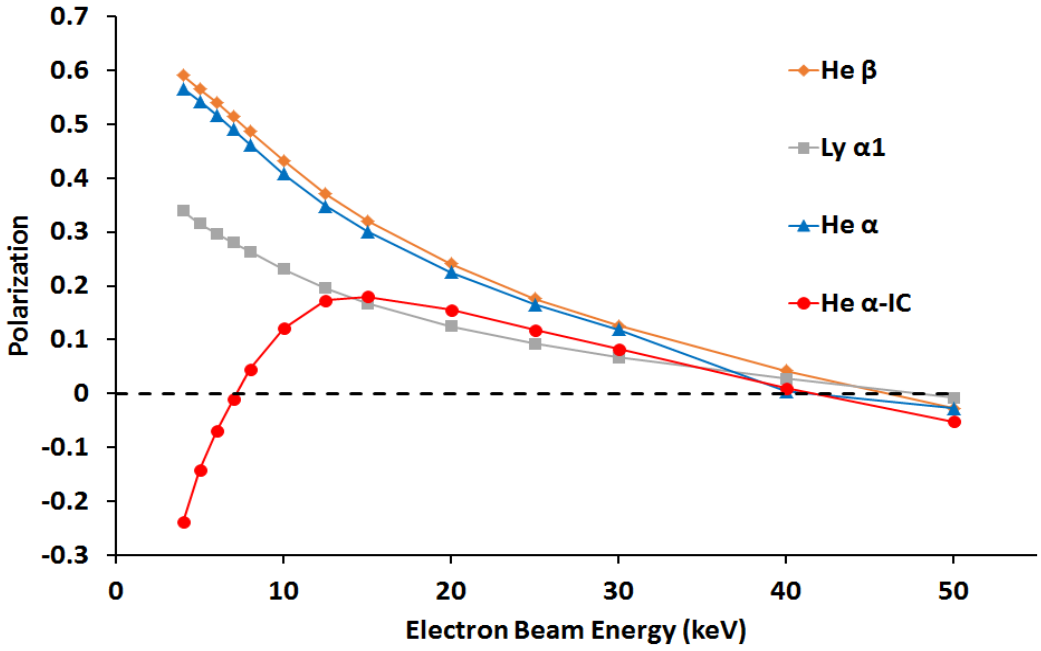

Fig. 4 Values of the degree of polarization of select He-like and H-like lines of argon. The polarization is a function of the electron beam energy and varies between roughly 3 keV to 50 keV.

It is important to mention first that the polarization of the Ly-α2 line is always zero. This is an intrinsic property of this line, and is due to the fact that the total angular momentum of this line is j = ½. The possible magnetic sublevels are therefore m_j = -½ and ½. Since there is no possible way to preferentially populate a sublevel, the polarization will always be zero. This indicates that the Ly-α doublet is an ideal candidate for PPS since one of the two lines is intrinsically unpolarized. If the resolving power of a spectrometer is not high enough, there are other possible combinations of lines that may be used. Although the polarization of no other line is zero, nor does any other candidate have a degree of polarization that remains relatively flat as a function of the electron impact energy, several useful facts are observed. In particular, the degree of polarization of the He-α and He-β lines is positive at low electron impact energies, and tends to zero with increasing impact energy. On the other hand, the He-α IC line is negatively polarized at lower electron beam energies, tends to increase quite quickly until roughly 15 keV, and proceeds to level off and approach zero like the other lines. This is a useful feature to diagnose the electron beam energy. If one measures, for example, the polarization of the He-α and He-α IC lines, one can infer that the electron beam energy is relatively low if the two degrees of polarization differ greatly, or the electron beam energy is quite high if both lines have a comparable degree of polarization. A similar argument may be made if one chooses to use the He-β and He-α IC lines.

The calculations presented thus far are for an idealized case where the degree of polarization is maximized due to an EDF consisting solely of non-thermal electrons. In a DPF, however, the EDF will largely consist of thermal (Maxwellian) electrons with a small tail of non-Maxwellian electrons. In Figs. 5, 6 and 7, a set of results from a new magnetic sublevel kinetics code are presented. All results are catered to represent data for the most accessible line candidates,

namely the He-like transitions discussed above. All spectra presented in these figures were broadened with a Voigt profile. In Fig. 5, a set of simulations were run for He-like argon ions where the fraction of fast electrons was varied from 0% to 100%. The EDF of the fast electrons is set as a Gaussian. The synthetic spectra are all normalized to unity. The electron temperature was set to T_e = 750 eV, the electron density was set to $n_e = 1x10^{19}cm^{-3}$, and the fast electrons were centered at an energy of 5 keV with a full width at half maximum of 50 eV.

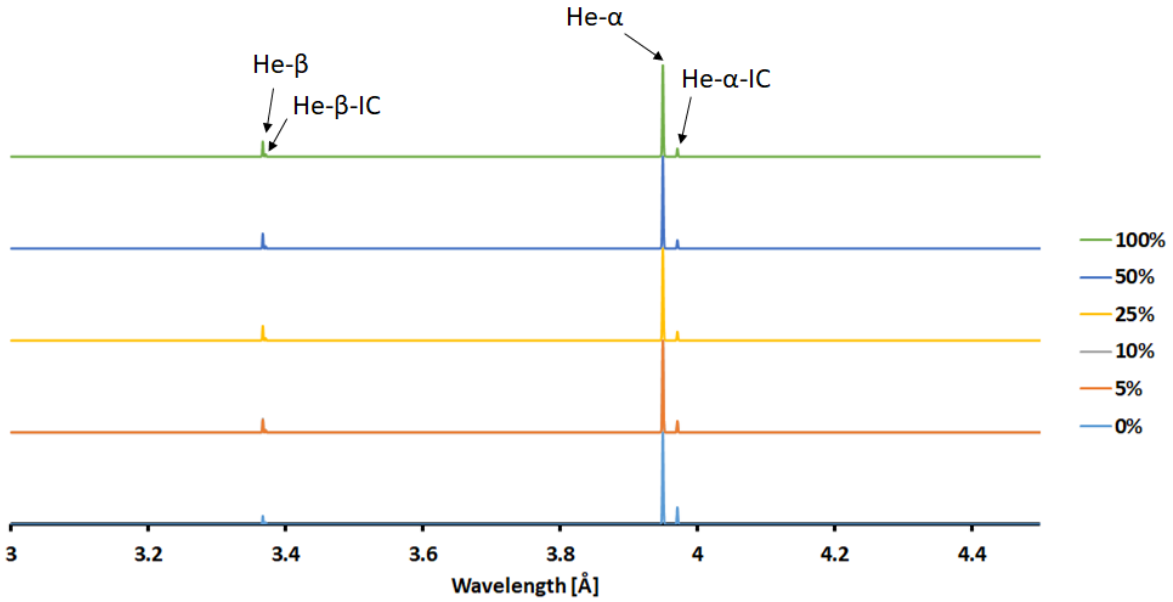

Fig. 5 Synthetic spectra produced using the new magnetic sublevel kinetics code. The fraction of hot electrons is varied from 0% to 100%. The electron temperature for each simulation as T_e = 750 eV and the electron density was $n_e = 1x10^{19}cm^{-3}$. The EDF is Gaussian and centered at an energy of 5 keV with a full width at half maximum of 50 eV.

As the fraction of fast electrons is increased, the intensity of the He-α IC line decreases and the intensities of the He-β and He-β IC line increases. Thus the relative intensities of these lines can be used as a diagnostic for estimating the percentage of non-thermal electrons in plasmas. In Fig. 6, the intensity of the lines as a function of the electron energy is illustrated. In this case, the fraction of fast electrons was set to 100% and the center of the Gaussian function was varied between 4 keV and 15 keV.

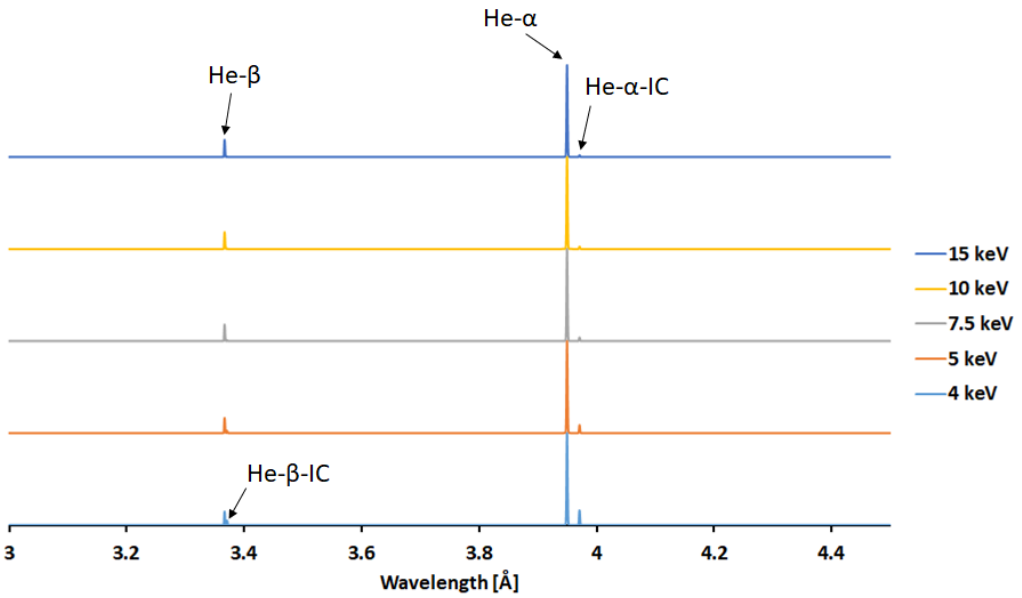

Fig. 6 Synthetic spectra produced using the new magnetic sublevel kinetics code. The fraction of fast electrons is kept at 100% and the center of the Gaussian EDF is varied between 4 – 15 keV.

In a fashion similar to the results observed in Fig. 5, the He-α IC, He-β IC, and He-β lines all show sensitivity to a variation in the energy. This supports the notion that they can be used as a diagnostic for inferring the energy of an electron beam. Finally, in Fig. 7, calculations of the degree of polarization of the lines mentioned above are presented. These populations are calculated using the magnetic sublevel populations in accordance with Eq. (3). The fraction of fast electrons is kept at 100% for comparison purposes. Overall, there is an excellent match between the results produced using the new code, and those produced using the polarization module of FAC.

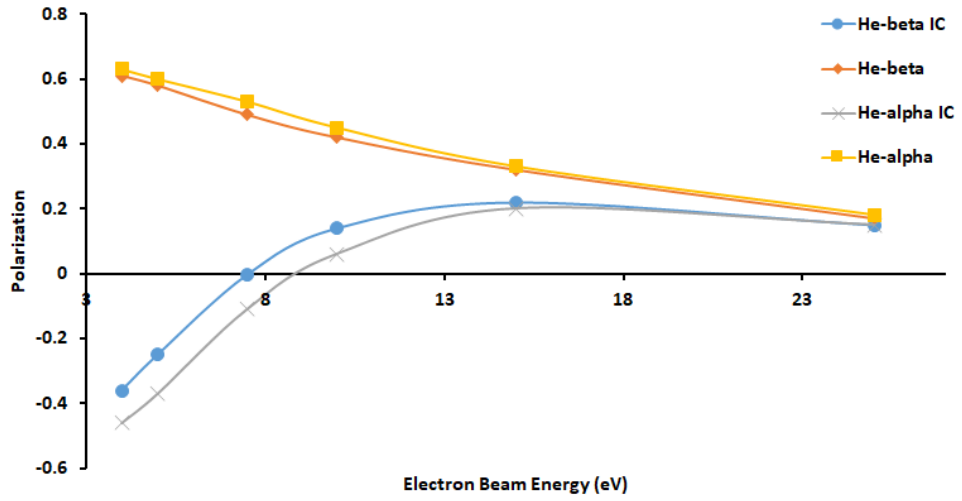

Fig. 7 Calculations of the degree of polarization of several He-like lines produced using the new magnetic sublevel kinetics code.

In Fig. 8, data from an MHD simulation using the Athena code is presented. This simulation used argon as a dopant in the center gas puff conductor and deuterium in the Marshall guns. The simulation was performed to get an estimate of the overall plasma temperature and mass density.

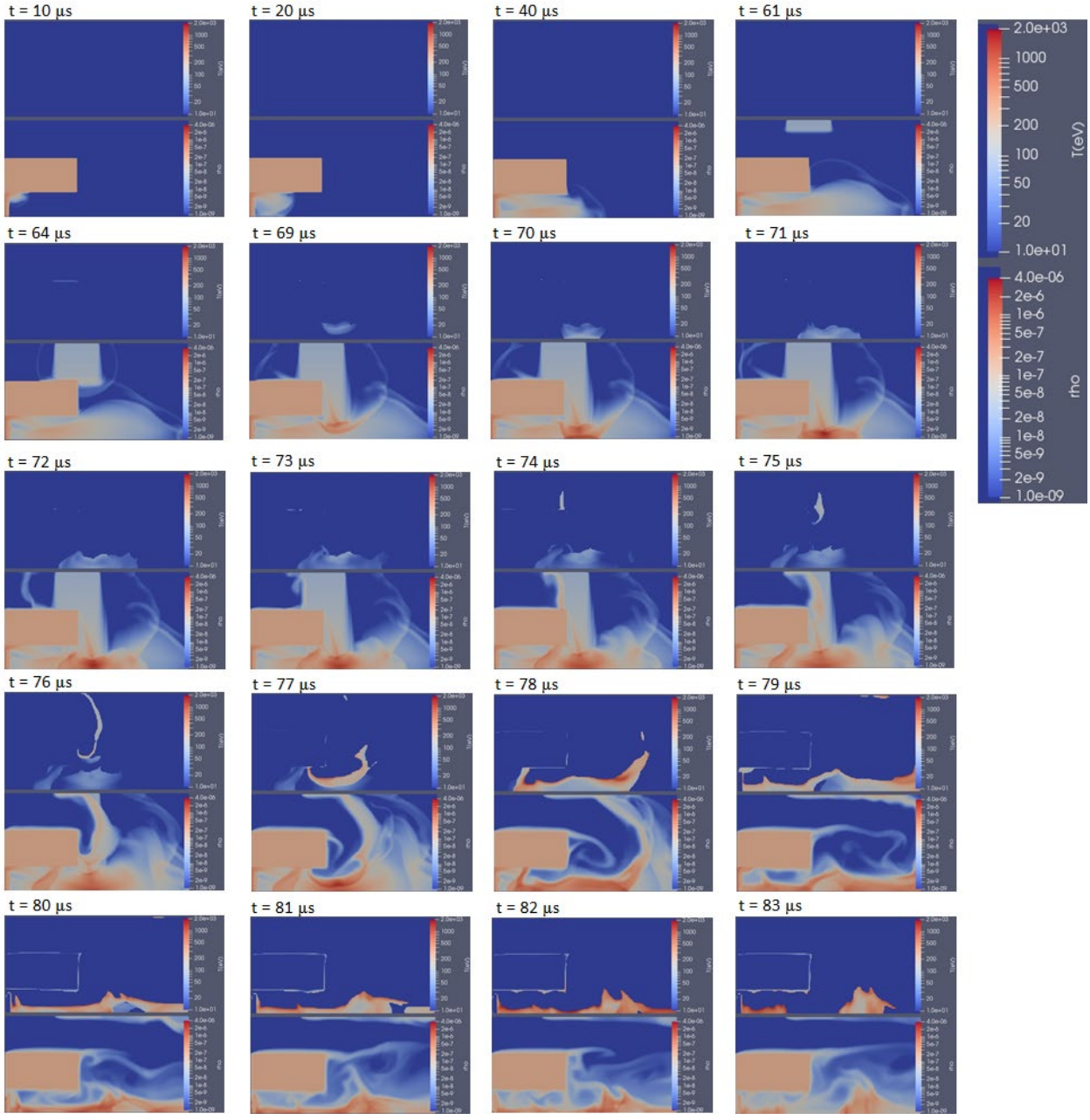

Fig. 8 Simulations of the plasma temperature (top half of figure at each time step) and mass density (bottom half) of an Ar doped deuterium shot on Hawk using the MHD code Athena. The scale has been enlarged for visual purposes.

Based on these calculations, it is estimated that after the deuterium plasma compresses the neutral argon injected by the gas puff, the highest plasma temperature achieved is on the order of 2 keV. Although this single-temperature estimate represents the total temperature of the whole volume of

plasma, it is reasonable to expect that the plasma electron temperature reaches sufficiently high values to produce K-shell Ar radiation.

The details of the experimental efforts are summarized next. First, a test was done to ensure that argon dopant was successfully injected into the chamber. Figure 9 shows a visible spectrum collected under two different conditions. In the left graph, the Marshall guns used to inject deuterium plasma into the chamber and the center conductor gas puff is triggered to also inject neutral gas, however the Marx bank is not fired. In the right graph, the same criteria are met, however now the Marx bank is discharged, and the two graphs are overlaid for comparison.

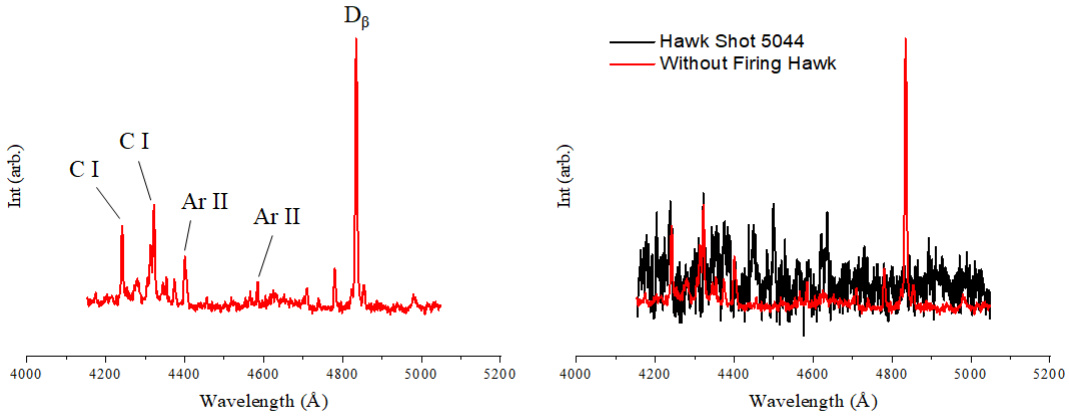

Fig. 9 Visible spectroscopy of experiments on Hawk using the Marshall guns and center gas puff conductor. Argon is added as a dopant via the gas puff and deuterium is injected into the chamber via the Marshal guns.

Line identification indicates the presence of singly ionized (Cl-like) argon ions as well as neutral carbon ions which are an impurity present within the chamber. Moreover, when examining the experiment where the Marx bank is not discharged, the deuterium Dβ line is observed. However, this signature disappears when the Hawk Marx bank is discharged. The neutral carbon signatures remain as well as very minimal amounts of the singly ionized argon atoms. In Fig. 10, a time-integrated pinhole camera image and the current and voltage traces are shown from Hawk shot 5044. The image in Fig. 10 shows x-rays from the plasma pinch as well as tungsten (W) radiation from the gas puff hardware and electrodes. The pinch is the main source of radiation from which the expected K-shell argon lines would be emitted and recorded by an x-ray crystal spectrometer.

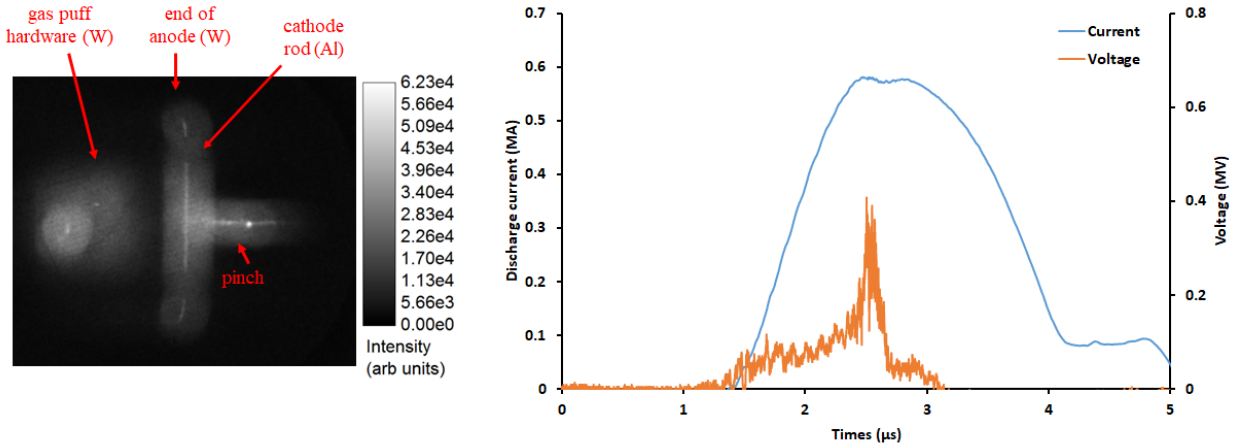

Fig. 10 Time-integrated x-ray pinhole camera image and current and voltage signals from Hawk shot 5044.

Several attempts were made to collect spectroscopic data using a convex crystal spectrometer with a KAP (2d = 26.632 Å) and Mica crystal (2d = 19.84 Å) with light sensitive film. Attempts were made using both argon and neon in the center gas puff conductor. Due to a high number of scattered hard x-rays, the initial attempts resulted in totally over-exposed films. The spectrometer was then wrapped in a layer of lead to provide shielding from the scattered hard x-rays. Subsequent experiments produced films with normal exposure, but no spectral lines were observed on the films. To troubleshoot the spectrometer, testing and optimization began off-line using an x-ray pulser. However, due to the Covid-19 pandemic, completion of the optimization and additional shots to collect spectroscopic data were indefinitely delayed.

2.4 Conclusions

Research was performed to investigate the generation physics of high-energy electron beams in high-energy-density plasmas. The research consisted of theoretical and experimental components.

Theoretical calculations were performed using the flexible atomic code (FAC) as well as several non-local thermodynamic (non-LTE) equilibrium kinetic models to identify line emission candidates for spectropolarimetry studies. Additional theoretical calculations were performed using the polarization module of FAC with a Gaussian electron distribution function to calculate the maximum degree of polarization of the suitable line candidates. These calculations showed that several He-like lines were suitable candidates, including the He-α, He-α IC, and He-β lines. Useful trends in the degree of polarization of these lines as a function of electron impact energy were observed. In particular, the intercombination lines have negative degrees of polarization at lower electron impact energies whereas the He-α and He-β lines have positive degrees of polarization at lower electron impact energies. This is a useful diagnostic for determining the electron beam energy in plasma.

A magnetic sublevel kinetics code was developed which can serve to calculate the degree of polarization and produce polarization sensitive spectra. The code is able to handle both a Maxwellian and Gaussian electron distribution function simultaneously. This is particularly useful since most HED plasmas consists largely of thermal electrons, with a small tail of fast electrons. Several synthetic spectra were generated and presented to examine the sensitivity of the lines to the fraction of fast electrons and the center energy of the Gaussian distribution function.

Radiative cooling rates for K-shell argon ions were calculated by the finite volume MHD code Athena and used to produce an estimate of the plasma electron temperature and mass density of a Hawk shot doped with argon gas. The single temperature of the plasma was estimated to reach up to 2 keV, which should be sufficient to ionize K-shell argon ions. Based on this fact, experiments were carried out on the Hawk pulsed-power generator with deuterium in the Marshall guns and argon in the center gas-puff valve. A pinhole camera was used to image the pinch, and an x-ray crystal spectrometer was used to attempt to collect time-integrate, spatially-resolved spectra. Due to background noise from hard x-ray radiation coming off of the chamber hardware, the initial shots resulted in overexposed film. The spectrometer was wrapped in lead shielding to reduce background noise, and subsequent shots produced film with normal exposure amounts, but no x-ray emission lines. The spectrometer was then removed from the chamber for off-line testing using an x-ray pulser. Due to the Covid-19 pandemic, further optimization of the spectrometer and additional shots on Hawk were indefinitely delayed. Additional experiments in the future would be beneficial in order to measure the electron temperature of a shot on Hawk with argon or neon in the center gas puff. Based on those results and the intensity and availability of K-shell spectral lines, a spectropolarimeter can be developed to provide further insight into the energy of the electron beam produced by a dense plasma focus.

3. ACKNOWLEDGEMENTS

This research was supported by the Naval Research Laboratory Karles Fellowship program. The authors also acknowledge and are thankful for the assistance from Joseph T. Engelbrecht and Brian J. Sobocinski in fielding the crystal spectrometer and x-ray pinhole cameras during the Hawk DPF experiments.

4. REFERENCES

1. M. Milanese, R. Moroso, and J. Pouzo, “D-D neutron yield in the 125 J dense plasma focus Nanofocus”, Eur. Phys. J. D **27**, 77 (2003).
2. D. Wong, A. Patran, T. L. Tan, R. S. Rawat, and P. Lee, “Soft x-ray optimization studies on a dense plasma focus operated in neon and argon in repetitive mode”, IEEE Trans. Plasma Sci. **32**, 2227 (2004).
3. M. F. Gu, “The Flexible Atomic Code”, Can. J. Phys. **86**, 675 (2008).
4. J. M. Stone, T. A. Gardiner, P. Teuben, J. F. Hawley, and J. B. Simon, “Athena: A new code for astrophysical MHD,” Astrophys. J. Suppl. Ser., vol. **178**, pp. 137–177, Sep. (2008).
5. J. Marshall, “Performance of a hydromagnetic plasma gun,” The Physics of Fluids, vol. **3**, no. 1, pp. 134–135, (1960).
6. S.B. Hansen, PhD Dissertation, University of Nevada, Reno (2003).
7. N. D. Ouart, P. W. L. de Grouchy, N. Qi, J. L. Giuliani, A. Dasgupta, T. A. Shelkovenko, S. A. Pikuz, D. A. Hammer, B. R. Kusse, J. P. Apruzese, and R. W. Clark, “Radiative properties of argon gas puff z-pinch implosions on COBRA”, Phys. Plasmas. **23** 101202 (2016).